3D coordination polymers constructed from d^{10} metal ions, flexible 1,2,4-triazole derivatives and aromatic tetracarboxylates: Syntheses, structures, thermal and luminescent properties

Leila Heidari [a], Mitra Ghassemzadeh [a,*], Dieter Fenske [b], Olaf Fuhr [b], Farshid Mohsenzadeh [a], Volodymyr Bon [c]

[a] *Department of Inorganic Chemistry, Chemistry & Chemical Engineering Research Center of Iran, Pajoohesh Blvd., 17th Km of Tehran–Karaj Highway, Tehran, 14968-13151, Iran*

[b] *Institut für Nanotechnologie and Karlsruhe Nano Micro Facility (KNMF), Karlsruher Institut Für Technologie, Hermann-von-Helmholtz-Platz 1, 76344, Eggenstein-Leopoldshafen, Germany*

[c] *Department of Chemistry, Technische Universitat Dresden, Bergstraße 66, 01069, Dresden, Germany*

ARTICLE INFO

Keywords:
Coordination polymers
3-Mercapto-1,2,4-Triazoles
Zinc(II) complex
Cadmium(II) complex
Mixed-ligand system
Pillar−layered structures

ABSTRACT

The reaction of mixed-ligands 1,2,4,5-benzene tetracarboxylic acid (H_4btec) and 1,2-*bis*(4-amino-5-methylmercapto-1,2,4-triazole-3-yl)ethane (bamte) with zinc(II) nitrate hexahydrate under hydrothermal conditions led to the formation of the coordination polymer $[Zn_2$ (bamte) (btec)$]_n$ (**CP1**), whereas the reaction of the same organic tetraacid with 4-amino-5-(pyridine-4-yl)-4*H*-1,2,4-triazole-3-thiol (Haptt) and cadmium (II) nitrate tetrahydrate under solvothermal conditions gave the coordination polymer $[Cd_3$ (aptt)$_2$ (btec)$]_n$ (**CP2**). Both CPs have been characterized by elemental analysis, FT IR, powder X-ray diffraction as well as single-crystal X-ray diffraction. Both complexes possess three-dimensional (3D) networks based on two-dimensional M^{II}-btec^4 - layers connected by multidentate triazole moieties. **CP1** shows a rarely observed binodal (4,6)-connected "*fsc*'' coordination network with $(4^4.6^{10}.8)$ $(4^4.6^2)$ topology, whereas **CP2** presents a new tetranodal (4,4,5,6)-connected 3D net with $(4^3.6^2.8)_2$ $(4^4.6^2)$ $(4^4.6^6)_2$ $(4^6.6^6.8^3)$ point symbol. Furthermore, the morphology, thermal stability, and solid-state luminescent property of both coordination polymers have been investigated.

1. Introduction

Over the past two decades, the synthesis of coordination polymers (CPs) has attracted increasing attention due to their fascinating structural diversity and potential applications in various fields, such as gas adsorption and storage, separation, sensors, luminescence, and catalysis [1 16].

It is often reported that such potential bulk properties of CPs are in direct relationship with their structural dimensions and network topology [17,18]. In general, the architecture of the final structure of CPs is affected by the nature and molar ratio of the reactants, template structure, pH and temperature, penchant of metal ions for a specific coordination geometry, and counter anions [19 26].

In particular, the organic linkers with the number and orientation of the donor groups, rigidity, or flexibility as well as their length play a vital role in determining the nature of CPs. Indeed, these linkers serve to exert influence on the degree of their dimension, interpenetration, topology, as well as their porosity [27,28]. In that respect, the use of a so called "mixed ligand system" a combination of organic compounds containing donor atoms such as nitrogen, oxygen, sulfur has proven to be an effective strategy for the design, synthesis, and regulation of CPs [29 31]. Multi carboxylic acids as one part of the mixed ligand systems constitute one of the most widely utilized oxygen donor organic classes since carboxylates have the ability to coordinate to metal centers in diverse modes (monodentate, bridging, and chelating) [32,33]. On the other hand, the N donor heterocyclic compounds such as pyridine, imidazole, pyrazine, and triazole derivatives have been broadly used as another part of the mixed ligand system acting as molecular building blocks or co ligand in the construction of CPs [34 37]. Amongst the N donor heterocyclic compounds, the coordination behavior of 1,2,4 triazole may be regarded as a combination of coordination geometries of both pyrazoles and imidazoles. Thus, they have the ability to act as a

* Corresponding author.
E-mail addresses: mghassemzadeh@ccerci.ac.ir, m.ghassemzadeh@yahoo.de (M. Ghassemzadeh).

monodentate ligand or bridging agent between metal ions resulting in the formation of mono , bi or polynuclear complexes. Furthermore, the variety of these coordination modes can be extended by introducing further functional groups into the 1,2,4 triazole core. For instance, 4 amino 3 mercapto 1,2,4 triazole possess the ability to coordinate to metal ions as N or S monodentate, N,S chelating, N,N and, N,N,S bridging ligand. Recently, we have reported the synthesis and characterization of various mono or binuclear late transition metal complexes (e.g., Cu(I), Cu(II), Ag(I), and Pd(II)) containing 1,2,4 triazole derivatives under conventional conditions [38 42]. For example, we synthesized a new silver(I) coordination polymer $[\{[Ag(L1)]NO_3\}_2]_n$ containing 4 amino 3 ethyl 1*H* 1,2,4 triazole 5(4*H*) thione (L1). According to the determined molecular structure, the ligand acts as a bridging agent between metal centers using its sulfur and nitrogen atoms, representing an unprecedented coordination mode. This coordination mode leads to the formation of a 10 membered Ag S "mosaic'' pattern and causes a two dimensional (2D) endless framework [38]. Moreover, we have synthesized the first dinuclear metallacyclic Cu(I) complexes based on a *bis* triazole derivative, namely $[Cu_2(L2)_2(X)_2]$ (L2 4,4' ((1Z, 1′Z) ((((1, 2 phenylene*bis* (methylene))*bis* (oxy))*bis* (2,1 phenylene))*bis* (methanylylidene))*bis* (azanylylidene))*bis* (3 methyl 1*H* 1,2,4 triazole 5(4*H*) thione), X Cl and I), in which each ligand acts as bridging agent between two Cu X units *via* the sulfur atoms of its 1,2,4 triazole heterocycles [40]. We have also reported the synthesis and molecular structure of various mono and dinuclear palladium (II) complexes containing 1,2,4 triazole derivatives [41,42]. For instance, the mononuclear palladium (II) complex $[Pd(L3)_2]Cl_2 \cdot 4CH_3CN$ was obtained by the reaction of *bis* 1,2,4 triazole derivative, 5,5' (1,3 phenylene*bis* (methylene)) *bis*(sulfanediyl)*bis* (3 methyl 4H 1,2,4 triazol 4 amine) (L3) with palladium (II) chloride [42]. The molecular structure of the complex revealed that the ligands are coordinated through the four N1 atoms of the four 1,2,4 triazole moieties. This coordination mode led to the formation of a spiro metallocyclic complex of palladium (II). In addition, the chemistry of building blocks containing two 1,2,4 triazole units has also been investigated for the preparation of CPs displaying intriguing topologies and interesting properties [43]. Despite a number of reports dealing with the synthesis of CPs from N alkyl or aryl substituted *bis* 1,2,4 triazoles, their preparation from C3 alkyl substituted *bis* 1,2,4 triazoles remains scarce [44 47].

Taking into account the importance of 1,2,4 triazoles in coordination chemistry and our ongoing interest in the development of their complexes (as well as investigation of their coordination mode to novel metal ions), our research group has focused on the structure and properties of CPs based on 1,2,4 triazole derivatives. The aim of this study is to construct d^{10} coordination polymers containing mixed ligand systems, including 3 mercapto 1,2,4 triazole derivatives as N and/or S donor polydentate building blocks and benzene tetracarboxylates as linkers. In this regard, two novel 3D coordination polymers of zinc(II) and cadmium (II) ion based on flexible 1,2,4 triazole derivatives, namely 1,2 *bis*(4 amino 5 methylmercapto 1,2,4 triazole 3 yl)ethane and 4 amino 5 (pyridine 4 yl) 4*H* 1,2,4 triazole 3 thiol, have been synthesized under hydrothermal or solvothermal conditions, respectively. According to the results of our experiments, both solvo and hydrothermal conditions were found to be beneficial methods for the preparation of these complexes since cadmium (II) nitrate or zinc(II) nitrate underwent no reaction with the corresponding 1,2,4 triazoles under conventional or reflux conditions. Furthermore, the thermal stability and the luminescence properties of both CPs were investigated.

2. Experimental section

2.1. Materials and instruments

All other starting materials and solvents, except Haptt and 2 *bis* (4 amino 5 thio 1,2,4 triazol 3 yl) ethane, were obtained from Merck and Fluka and used as received without further purification. The synthesis procedure of Haptt and bamte are given in Supporting Information. FT IR spectra were recorded as KBr discs (4000 400 cm^{-1}) with a Perkin Elmer 400 spectrometer. Elemental analyses (C, H, and N) were performed on a PerkinElmer 2400 CHN Elemental Analyzer. Thermal gravimetric analyses (TGA) were carried out with a Netzsch TG 209F1 apparatus with a heating rate of 10 °C min^{-1} under an atmosphere of flowing air. SEM images were obtained using VEGA3 TESCAN and were carried out at an accelerating voltage of 20.0 kV. The powder X ray diffraction measurements were carried out using a Bruker D8 Advance diffractometer with a Cu anode that generated Cu K_α radiation (λ 1.5406 Å). Thermogravimetric analysis (TGA) was performed on a Mettler Toledo TGA/SDTA851e thermal analyzer (test conditions: air atmosphere and heating of the complex up to 900 °C with temperature program rate 10 °C min^{-1}). Photoluminescence measurements were performed on a PerkinElmer LS55 spectrofluorometer.

2.2. Synthesis of complexes

$[Zn_2(bamte)(btec)]_n$ (**CP1**). Bamte (0.050 g, 0.176 mmol), H_4btec (0.045 g, 0.176 mmol), triethylamine (0.10 mL, 0.704 mmol) were added to an aqueous solution (30 mL) of $Zn(NO_3)_2 \cdot 6H_2O$ (0.105 g, 0.353 mmol). The clear solution was kept in a sealed glass vial at 120 °C for 72 h then cooled to room temperature under ambient conditions. The obtained colorless crystals of **CP1** were filtered off, washed with distilled water (2 x 10 mL) and dried in air. Yield: 28% (based on bamte). Anal. Calc. for $C_9H_8N_4O_4SZn$ (%): C, 32.40; H, 2.42; N, 16.79; Found (%): C, 32.16; H, 2.33; N, 16.50. FT IR (KBr, ν, cm^{-1}): 3304 (w, $\nu_{N\ H}$), 3186 (w, $\nu_{N\ H}$), 1611 (s, $\nu_{C\ N}$), 1581 (s), 1497 (s), 1420 (s), 1374 (s), 1137 (m), 923 (w), 870 (w), 816 (m), 763 (w), 675 (w, $\nu_{C\ S}$), 621 (m), 522 (w).

$[Cd_3(aptt)_2(btec)]_n$ (**CP2**). $Cd(NO_3)_2 \cdot 4H_2O$ (0.224 g, 0.72 mmol) and H_4btec (0.0455 g, 0.18 mmol) were added to a warm solution of Haptt (0.07 g, 0.36 mmol) in EtOH/H_2O (40 mL, 1:1) and was stirred for 5 min. The mixture was kept in a sealed glass vial at 100 °C for 72 h, cooled to room temperature under ambient conditions and the precipitated colorless block crystals of **CP2** were collected by filtration, washed with distilled water (2 x 10 mL), and dried in the air. Yield: 38% (based on Haptt). Anal. Calc. for $C_{24}H_{14}Cd_3N_{10}O_8S_2$ (%): C, 29.66; H, 1.45; N, 14.41; Found (%): C, 30.12; H, 1.49; N, 14.56. FT IR (KBr disc, cm^{-1}): 3452 (w), 3204 (w, $\nu_{N\ H}$), 2960 (w), 1628 (m), 1620 (m, $\nu_{C\ N}$), 1557 (s), 1478 (m), 1435 (m), 1364 (s), 1309 (m), 1218 (w), 1147 (w), 1060 (w), 1045 (w), 610 (w), 859 (w), 840 (w), 816 (w), 745 (w, $\nu_{C\ S}$), 686 (w), 658 (w), 580 (w), 526 (w).

2.3. Crystal structure determination and topological analysis of *CP1* and *CP2*

The selected crystals of bamte, **CP1**, and **CP2** were covered with perfluorinated oil and mounted on a STOE StadiVari single crystal diffractometer (Ga K_α radiation, λ 1.34143 Å). The orientation matrix and the unit cell dimensions were determined from 10 145 (bamte), 12 631 (**CP1**), and 36 357 (**CP2**) reflections, respectively. Using Olex2 [48], the structure was solved with the ShelXT [49] structure solution program using Intrinsic Phasing and refined with the ShelXL [50] refinement package using Least Squares minimization. All non hydrogen atoms were refined with anisotropic displacement parameters; the hydrogen atoms in **CP1** were modeled on idealized positions, whereas those in **CP2** could be localized and were refined freely. It is noteworthy to mention that there are two solvent molecules (ethanol) in the packing of **CP2**, which are masked by Olex2 due to their strong disorder. Crystallographic data collection and structure refinement parameters of **CP1** and **CP2** are summarized in Table 1. Solvent masks information for **CP2** is summarized in Table ST2 (Supporting Information). Topological analyses for **CP1**, and **CP2** were performed using the program package TOPOS 4.0 Pro [51].

[a]w $1/[\sigma^2(F_o^2) + (0.0427 \cdot P)^2 + 0.5571\ P)]$; P [max $(F_o^2, 0) + 2 \cdot F_c^2]/3$ and [b]w $1/[\sigma^2(F_o^2) + (0.0323 \cdot P)^2 + 3.5877\ P)]$; P [max $(F_o^2, 0) +$

Table 1
Summary of crystal data and structure refinement parameters for **CP1** and **CP2**.

	CP1	CP2
Empirical formula	$C_9H_8N_4O_4SZn$	$C_{24}H_{14}Cd_3N_{10}O_8S_2$
Formula weight	333.62	971.77
Temperature/K	180	180
Crystal system	triclinic	monoclinic
Space group	*P*1	$P2_1/c$
a/Å	8.012 (7)	10.879 (2)
b/Å	8.774 (8)	16.530 (2)
c/Å	9.479 (9)	8.6024 (2)
α/°	78.166 (7)	90
β/°	69.082 (7)	111.610 (1)
γ/°	70.165 (7)	90
Volume/$Å^3$	582.76 (10)	1438.14 (5)
Z	2	2
ρ_{calc}g/cm^3	1.901	2.244
μ/mm^{-1}	3.015	13.073
F (000)	336.0	936.0
Crystal size/mm^3	0.18 × 0.17 × 0.14	0.29 × 0.26 × 0.04
Radiation	Ga K_α (λ = 1.34143)	Ga K_α (λ = 1.34143)
2Θ range for data collection/°	8.73 to 125.024	8.918 to 125
Index ranges	$-9 \le h \le 10$	$-14 \le h \le 13$
	$-4 \le k \le 11$	$-21 \le k \le 21$
	$-12 \le l \le 12$	$-4 \le l \le 11$
Reflections collected	7140	20 433
Independent reflections	2755 [R_{int} = 0.0142, R_{sigma} = 0.0113]	3482 [R_{int} = 0.0174, R_{sigma} = 0.0102]
Indep. refl. with I ≥ 2σ (I)	2630	3448
Data/restraints/parameters	2755/0/174	3482/0/242
Goodness-of-fit on F^2	1.042	1.072
Final R indexes [I ≥ 2σ (I)]	R_1 = 0.0265, wR_2 = 0.0723[a]	R_1 = 0.0248, wR_2 = 0.0619[b]
Final R indexes [all data]	R_1 = 0.0277, wR_2 = 0.0731	R_1 = 0.0251, wR_2 = 0.0621
Largest diff. peak/hole/e $Å^{-3}$	0.81/-0.92	0.57/-1.07

$2 \cdot F_c^2]/3$. The crystallographic data have been deposited with the Cambridge Crystallographic Data Centre (CCDC) as supplementary publication numbers CCDC 2022962 (**CP1**) and 2 022 963 (**CP2**). Copies of the data can be obtained, free of charge, by application to CCDC, 12 Union Road, Cambridge, CB2 1EZ, UK (Fax: +44 1223 336033; Email: data request@ccdc.cam.ac.uk or *via* the internet: http://www.ccdc.cam.ac.uk/products/csd/request.

3. Results and discussion

3.1. Synthesis and characterization of complexes *CP1* and *CP2*

CP1 can be obtained from the reaction of bamte and H_4btec with zinc(II) nitrate hexahydrate in the presence of triethylamine under hydrothermal conditions as a white solid mass. **CP2** can be prepared by the reaction of Haptt and H_4btec with cadmium (II) nitrate tetrahydrate as a white crystalline solid (Scheme 1). Both coordination complexes are air stable.

3.2. Structural descriptions of *CP1* and *CP2*

Selected bond lengths and bond angles of bamte, **CP1**, and **CP2** are listed in Tables ST3, ST4, and ST5, respectively (Supporting Information). The hydrogen bonds of bamte, **CP1**, and **CP2** are summarized in Table ST6 (Supporting Information).

3.3. Crystal structure of $[Zn_2(bamte)(btec)]_n$ (*CP1*)

The coordination polymer **CP1** crystallizes in the triclinic system with space group *P*1. The compound consists of one Zn(II) ion, half of neutral bamte ligand, and half of the $btec^{4-}$ ligand (Fig. 1). The 3D framework of **CP1** viewing along *b* direction is depicted in Fig. 2a. In the structure of **CP1**, the fully deprotonated tetracarboxylate anion, $btec^{4-}$, acts as a μ_6 bridging ligand. Each of two *para* positioned carboxylates adopting *syn*

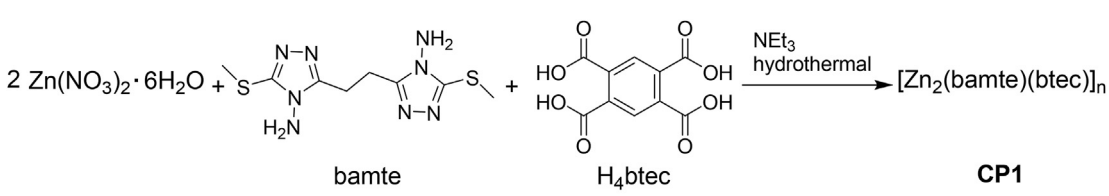

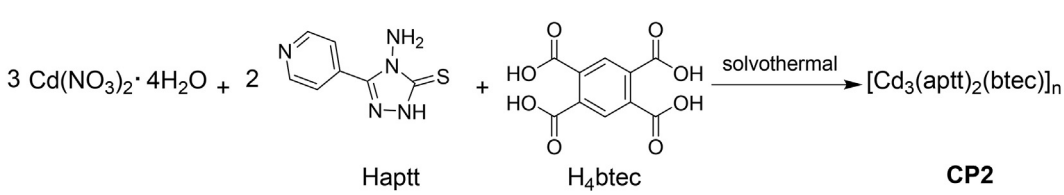

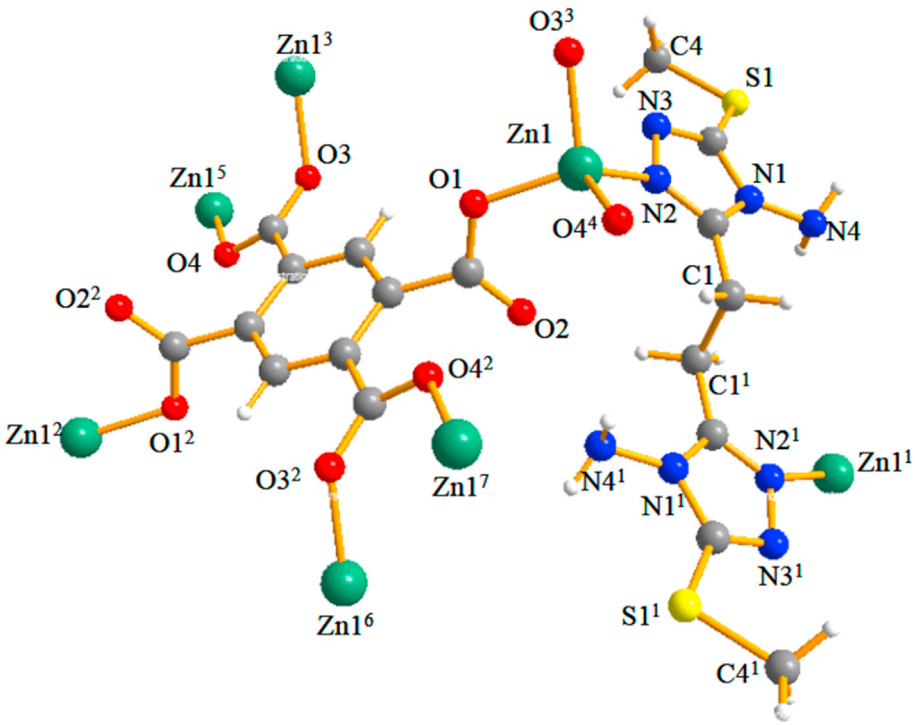

Fig. 1. A Stick-ball representation of a representative cutout of **CP1**.

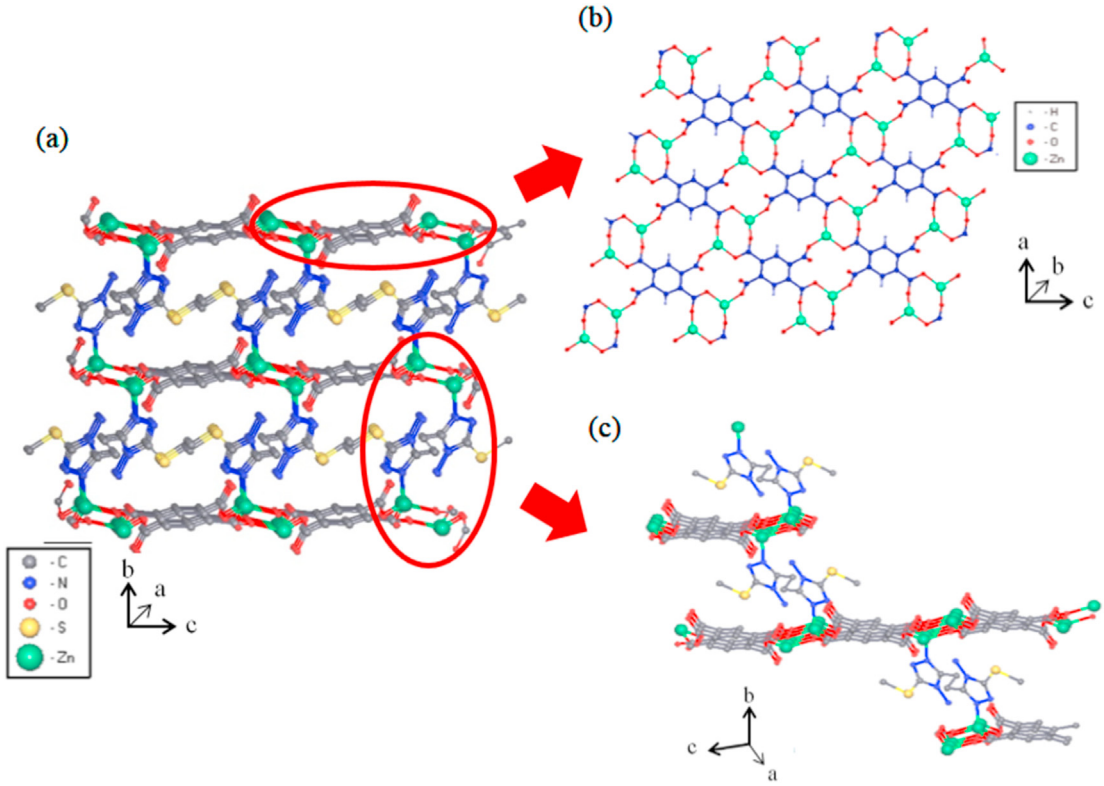

Fig. 2. (a) The 3D framework of **CP1** viewing along *a* direction, (b) the view of a 2D layer consisting of 8- and 16-membered rings along the *ac* plane, and (c) the representation of the coordination of bamte between the 2D layers.

syn η^1:η^1:μ_2 mode coordinate to two zinc ions (Zn1 O3^1: 1.968 (1) Å, Zn1 O4^2: 1.974 (1) Å, Zn···Zn$_{(syn\text{-}syn)}$: 3.79 (3) Å and Zn···Zn$_{(para)}$: 10.257 (1) and 11.098 (1) Å), whereas the other two *para* positioned ones showing monodentate coordination mode connect to two other zinc centers (Zn1 O1: 1.932 (1) Å and Zn···Zn: 10.965 (1) Å), resulting in the formation of wavy 2D layers parallel to the crystallographic plane *ac*. Each layer consists of alternately connected 8 and 16 membered rings (Fig. 2b). Moreover, the five membered heterocycles of bamte moieties

adopting *trans* configuration act as bridging agents (pillars along *b* axis) and connect the formed 2D layers into a 3D pillar layered framework with a Zn···Zn distance of 7.739 (9) Å (Fig. 2c).

They link two adjacent zinc atoms of one layer alternately to the zinc centers of the upper and the lower layers *via* their endocyclic hydrazinic nitrogen atoms (Zn1 N2: 1.984 (1) Å) and thereby complete the distorted tetrahedral geometry around each metal center (ZnO3N system, O1 Zn O3^1: 102.33 (5) °, O1 Zn O4^2: 102.83 (5) ° O3^1 Zn N2: 100.89 (5) ° and O4^2 Zn N2: 112.20 (5) °). All Zn O, and Zn N bond lengths are in the same range observed in other zinc(II) complexes involving fully deprotonated btec moieties and nitrogen donor heterocycles [47,52 57]. Interestingly, the distance between the best planes of the triazole moi eties of each bamte ligand of 1.779 (2) Å demonstrates well the flexibility of the bamte ligand in the complex (the distance between those in the free ligand is 0.307 (2) Å, Supporting Information). The 3D pillar layered structure is further stabilized *via* hydrogen bonds between the amine groups of the pillars and the oxygen atoms of the layers (N4 H4A ··· O1: 2.900 (2) Å and N4 H4A O1: 149.4 (1) °).

In order to gain a better insight into the 3D framework of **CP1**, a topological analysis was carried out. By topological analysis, the dinu clear secondary building units [$Zn_2(COO)_2$] and btec^{4-} ligands can be considered as a 4 connected and 6 connected node, respectively, while the bamte ligands are simplified as linkers. The overall 3D framework can be described as a binodal (4,6) connected *fsc* or *sqc11* topological network with the ($4^4.6^{10}.8$) ($4^4.6^2$) Schlafli symbol. Further analysis by TOPOS 4.0 Pro software reveals the vertex symbols ($4.4.4.4.6_2.6_2$) for each 4 connected node and ($4.4.4.4.6_2.6_2.6_5.6_5.6_5.6_5.6_5.6_5.6_5.8_{20}$) for each 6 connected node (Fig. 3).

Single crystal X ray analysis of **CP2** reveals that the coordination complex crystallizes in the monoclinic system with a $P2_1/c$ space group. The asymmetrical unit of **CP2** contains two crystallographic independent Cd(II) ions (Cd1 and Cd2 have 1/2 and 1 site occupancy, respectively), half of btec^{4-} anion and one singly deprotonated aptt moiety (Fig. 4). In this complex, each fully deprotonated btec^{4-} anion acts as a six fold bridging ligand and coordinates to six cadmium ions. Two *para* posi tioned carboxylates adopting monodentate mode coordinate to two Cd1 ions in a *trans* fashion with respect to the benzene ring (Cd1 O1: 2.308 (2) Å, Cd1 O1^1: 2.308 (2) Å, Cd1 O3^2: 2.464 (2) Å, Cd1 O3^3: 2.464 (2) Å, Cd1···Cd1: 8.60 (2) Å). Furthermore, each of the other *para* positioned carboxylates acting as *syn syn* η^1:η^1:μ_2 bridging ligand as well as monatomic one link two adjacent Cd2 ions (Cd2 O4^1: 2.441 (2) Å, Cd2 O3^5: 2.374 (2) Å, Cd2···Cd2$_{(syn\text{-}syn)}$: 4.33(1) Å and Cd2···Cd2$_{(para)}$: 11.70(1) Å) and one Cd1 ion (Cd1···Cd1: 8.60 (1) Å, Cd1···Cd2: 4.219 (0) Å. The dihedral angle between the best planes of the *ortho* positioned carboxylate groups (COO^-) is 61.01 (1) °. These coordination modes lead to the formation of wavy two dimensional Cd(II) btec^{4-} layers along crystallographic plane *bc* (Fig. 5b and c), in which the benzene rings are tilted by 81.86 (1) ° with respect to each other. Finally, the Cd(II) btec^{4-} layers are linked together by the aptt moieties as pillars along *a* axis to generate a 3D framework structure (Fig. 5a). Between these layers, each singly deprotonated triazole moiety acts as a three fold bridging as well as a chelating agent between three metal ions using its thiolate sulfur atom, endocyclic hydrazinic and pyridinic nitrogen atoms and, amine group. The thiolate group of each aptt moiety acts as a bridging agent between two cadmium centers, resulting in the formation of a zig zag polymeric Cd S chain along the crystallographic axis *c* with the Cd···Cd distance of 4.336 (1) Å (Cd2 S1: 2.626 (6) Å and Cd2 S1^4: 2.595 (6) Å, Cd2 S1 Cd2^7: 112.30 (2) ° and S1 Cd2 S1^4: 163.08 (2) °). Furthermore, the NH_2 group of each aptt moiety chelates the cadmium ion coordinated by the own sulfur atom stabilizing the polymeric chain (Cd2 N4: 2.485 (2) Å). Moreover, the pyridinic nitrogen atom of each aptt ligand acts as a bridging agent between two Cd2 centers of two adjacent Cd S chains (Cd2 N5^6: 2.292 (2) Å). These coordination modes are responsible for the formation of strands. Moreover, two adjacent strands are linked together *via* the thioamidic nitrogen atoms of each aptt moiety over a third cadmium ion (Cd1), resulting in the formation of the layers consisting of 20 membered rings parallel to crystallographic plane *bc* (Fig. 5d, Cd1 N2: 2.255 (2) Å, Cd1 N2^1: 2.255 (2) Å and Cd···Cd distance of 6.227 (1) Å). It is found that the best planes of two adjacent triazole moieties are perpendicular to each other (91.75 (1) °), whereas the best planes of each triazole heterocycle and its own pyridine moiety are tilted by 32.45 (4) ° with respect to each other. The latter demon strates well the flexibility of 1,2,4 triazole derivative in this compound compared with the dihedral angle of 20.10 (6) ° and 17.70 (2) ° observed in free ligand and {[Cd (aptt) (ptt)] H_2O}$_n$, respectively [58,59]. All Cd S, Cd N, and Cd O bond lengths are in well agreement with those observed in other cadmium complexes containing sulfur, nitrogen, and fully deprotonated btec^{4-} anion [59 67]. While Cd1 is surrounded by a N_2O_4 system, the Cd2 is coordinated by a $N_2O_2S_2$ system. Therefore, each cadmium (II) ion is located in a distorted octahedral environment. Interestingly, each singly deprotonated 1,2,4 triazole ring shows *Hückel* aromaticity. Both five membered heterocycle and the benzene ring are stacked with a dihedral angle of 5.83 (5) °, and centroid to centroid distance of 3.325 (4) Å, indicating the presence of a strong π ··· π inter action (Fig. 6a) [68]. Furthermore, each NH_2 group acts as a bridging agent and links the oxygen atoms of two different btec^{4-} moieties *via* intermolecular hydrogen bondings (N4 H4A ··· O2: 2.899 (4) Å, N4 H4A O2: 139 (3) °, N4 H4B···O2: 2.814 (5) Å and N4 H4B O2: 162 (3) °, Fig. 6b). These interactions along with the observed π ··· π inter action might be responsible for further stabilization of the coordination polymer **CP2**.

Topologically, simplified underlying net of **CP2** is formed from 4 con nected Cd1 nodes, 5 connected Cd2 nodes, 6 connected btec^{4-} nodes, and 4 connected aptt nodes. Therefore, the network of **CP2** features a tetranodal 4,4,5,6 connected net with ($4^3.6^2.8$)$_2$ ($4^4.6^2$) ($4^4.6^6$)$_2$ ($4^6.6^6.8^3$) Schlafli symbol (Fig. 7), which is identified by TOPOS 4.0 Pro as a new framework topology. The structure consists of Cd btec^{4-} layers connected by 1,2,4 triazole pillars. The topology of the layers is "*mta*" in standard representation of valence bonded MOFs.

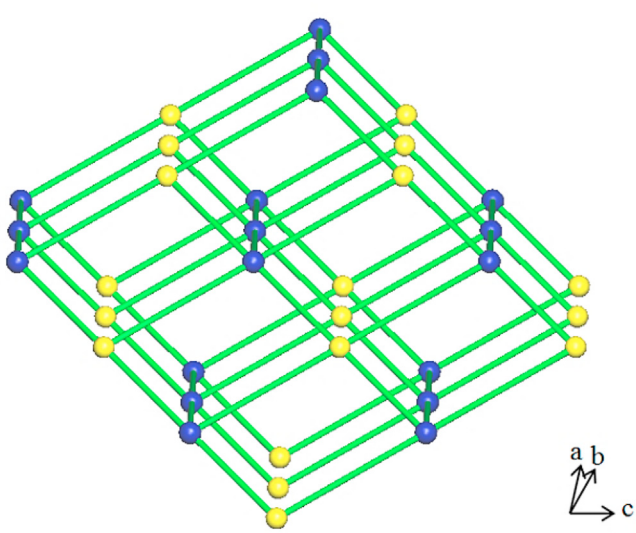

Fig. 3. The 3D *'fsc'* (4,6)-connected topological net with the Schläfli symbol of (4^4 6^2) (4^4 6^{10}·8) for **CP1**. Crystal structure of [Cd_3 (aptt)$_2$ (btec)] (**CP2**).

3.4. SEM images, PXRD patterns, and thermal gravimetric analyses of CP1 and CP2

To determine the morphological structures of the synthesized CPs, they were subjected to scanning electron microscope analysis (SEM). The SEM monographs of **CP1** show no specific shape (Fig. SF2, Supporting Information), while those of **CP2** exhibit the formation of spherical micrometric particles (Fig. SF3, Supporting Information).

In order to confirm the bulk purity of **CP1** and **CP2**, their powder X

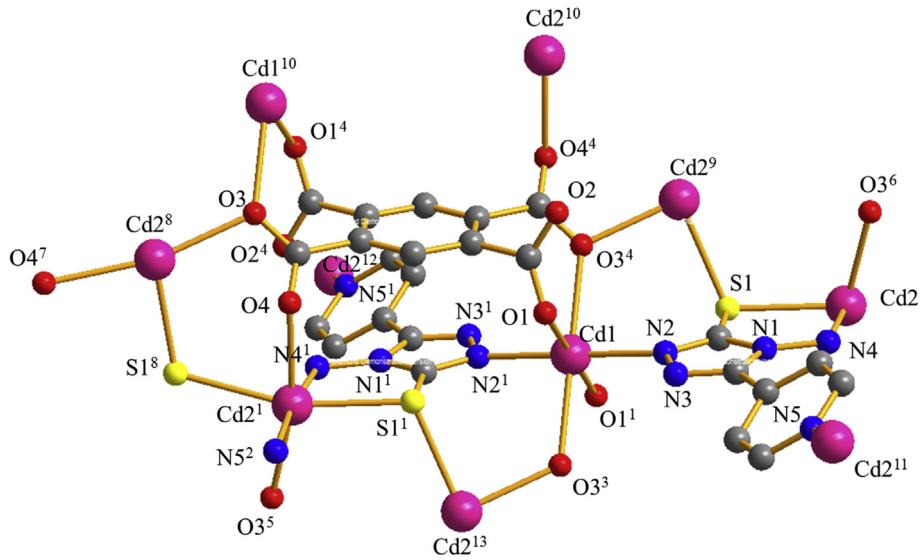

Fig. 4. Stick-ball representation of a representative cutout of **CP2**; all hydrogen atoms have been omitted for clarity.

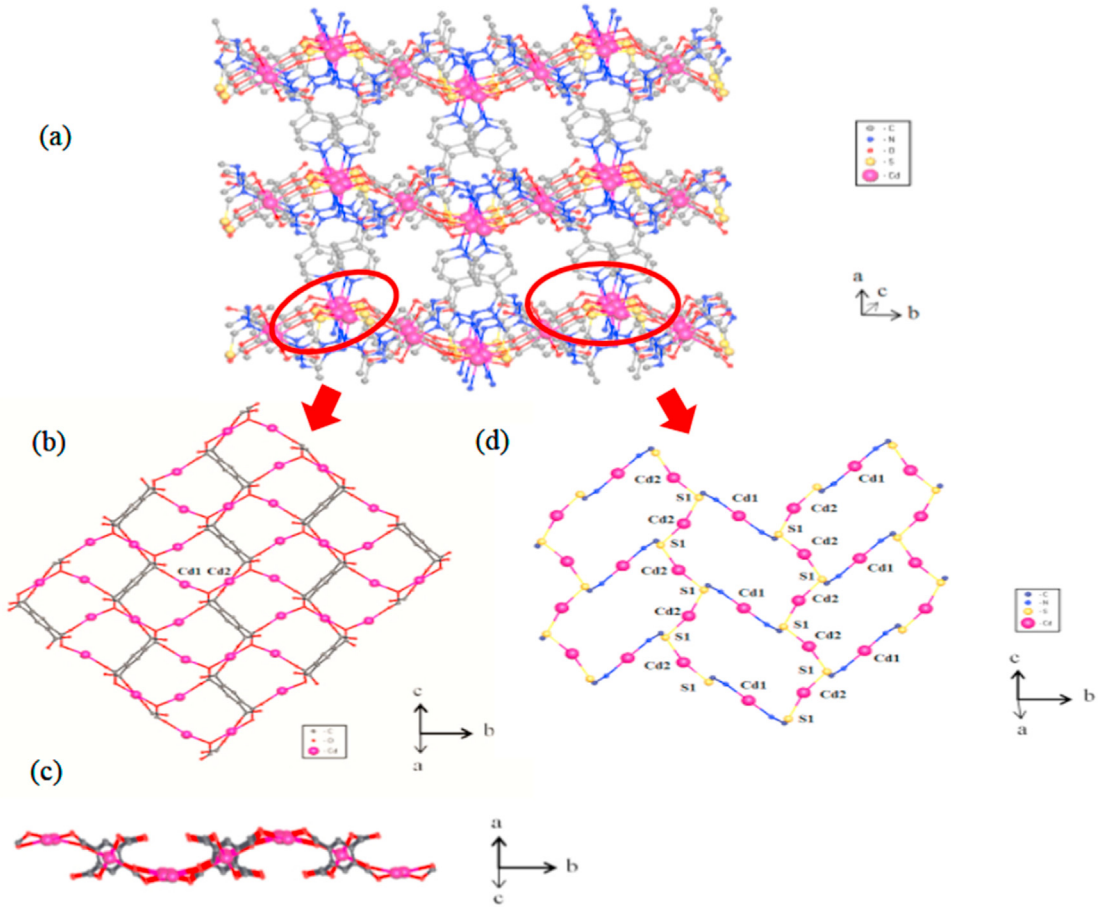

Fig. 5. (a) Representation of 3D framework of **CP2** viewing along *a* direction; (b) and (c) view of the wavy Cd(II)–btec^{4} layers along crystallographic plane *bc* and along *a* axis; (d) view of the layers consisting of 20-membered rings parallel to crystallographic plane *bc*.

ray diffraction patterns (PXRD) were recorded at room temperature and are depicted along with the simulated patterns generated from their single crystal data in figures SF4 and SF5 (Supporting Information). The patterns demonstrate the bulk phase purity of both CPs since their experimental patterns are in well agreement with the corresponding simulated ones. It is noteworthy to mention that the long term preservation of both compounds was also investigated. The XRD patterns of both compounds indicated that they remain unchanged even after being stored in air for a couple of months (figures SF6 and SF7, Sup porting Information).

In order to study the thermal stabilities of **CP1** and **CP2**, thermog ravimetric analysis was performed on both CPs in the temperature range

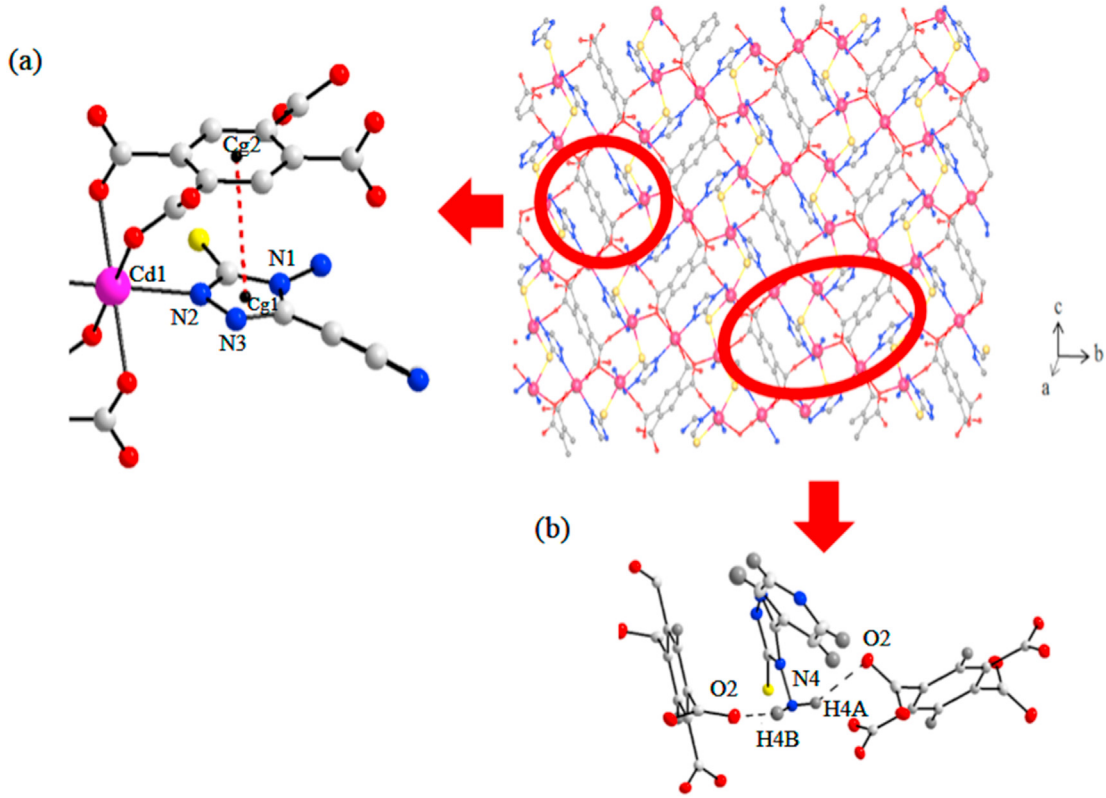

Fig. 6. Representation of stacked five-membered heterocycles and the benzene rings in **CP2** showing (a) the π ··· π interaction between five-membered heterocyclic ring and benzene ring and (b) hydrogen bonds (viewing along *a* direction).

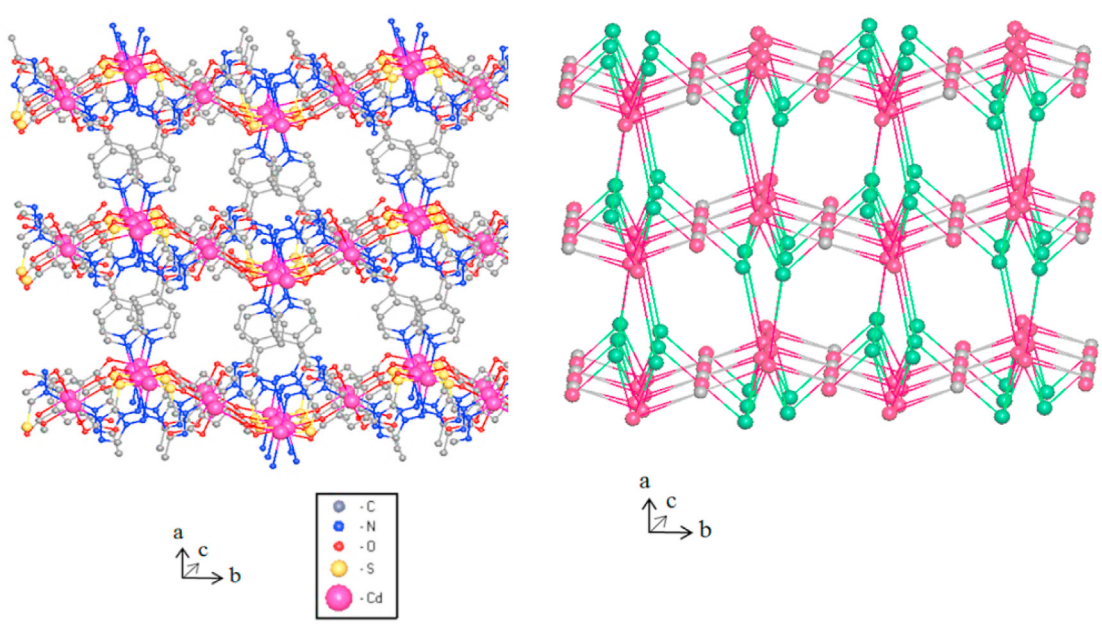

Fig. 7. Topological structure of **CP2** can be viewed as a 4-nodal (4,4,5,6)-connected net with $(4^3.6^2.8)_2$ $(4^4.6^2)$ $(4^4.6^6)_2$ $(4^6.6^6.8^3)$ Schläfli symbol.

of 30 900°C under an air atmosphere with a heating rate of 10 °C min^{-1} (Fig. 8). The differential scanning calorimetry/thermogravimetric analyses (TGA/DTG) of both CPs revealed that they have good thermal stability (decomposing temperature > 200 °C).

The spectra of **CP1** exhibit almost no weight loss below 280 °C (Fig. 8a). At T > 280°C, the framework starts to decompose gradually over three stages in the temperature range of 280 750 °C with a total weight loss of 76.63% corresponding to the removal of bamte (calculated: 42.9%), and $btec^{4-}$ (calculated: 32.7%). The residual product of **CP1** at 800 °C should be ZnO (found: 23.4% and calculated: 24.4%).

The spectra of **CP2** show a two stage thermal decomposition above 200 °C (Fig. 8b). The weight loss of 34.3% in the temperature range of 220 560 °C and of 31.0% in the range of 560 750 °C can be ascribed to the removal of solvent molecules, $btec^{4-}$ ligand (calculated: 34.7%), and

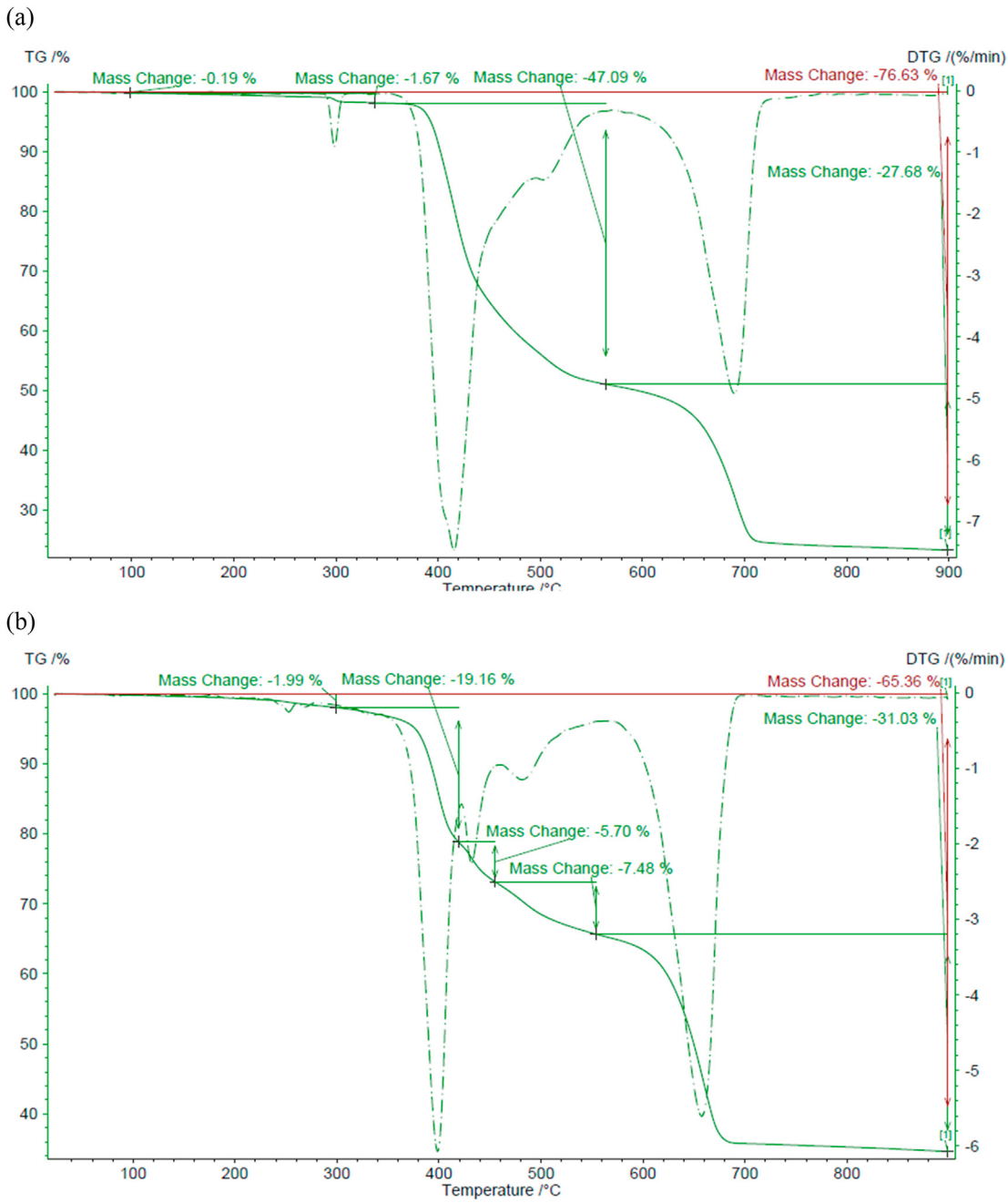

Fig. 8. (a) TGA/DTG plot of **CP1** and (b) TGA/DTG plot of **CP2**.

1,2,4 triazole moieties (calculated: 33.1%) in the framework. The remaining weight of 34.6% (calculated: 34.6%) indicates that the final product should be CdO.

To determine the chemical and morphological structure of the products from the thermogravimetric analysis of **CP1** and **CP2**, both coordination polymers were subjected to solventless thermolysis at 800 °C in air. The products from solventless thermolysis (sample **1** and sample **2**) were analyzed using energy dispersive X ray spectroscopy (EDX) and SEM. The EDX analyses of samples **1** and **2** confirmed that each sample consists of corresponding metal oxide (Figures SF8 and SF9, respectively, Supporting Information). The scanning electron micro graphs (SEM) of the samples show the formation of spherical particles of ZnO (mean diameter: ca. 90 nm) for sample **1** (Fig. SF10, Supporting Information) and spherical micrometric particles of CdO for sample **2** (Fig. SF11, Supporting Information).

3.5. *Luminescent properties of **CP1** and **CP2***

The luminescence of **CP1**, **CP2**, and free ligands were studied in the solid state at room temperature (Fig. 9). The emission bands can be observed at 340 nm and 366 nm (λ_{ex} 276 nm) for H_4btec, 420 nm (λ_{ex} 300 nm) for Haptt, and 400 nm (λ_{ex} 340 nm) for bamte. Generally, the emissions observed for these organic ligands can be attributed to the intra ligand charge transfer ($\pi^* \rightarrow n$ or $\pi^* \rightarrow \pi$ transitions) [69 71]. **CP1** shows a maximum emission band at 405 nm (λ_{ex} 340 nm) with a slight red shift and an increased intensity compared with that in the spectrum of free bamte. The emission spectra of **CP2** exhibit an emission peak at 410 nm upon excitation at 300 nm with a slight blue shift and an increased intensity compared to the corresponding 1,2,4 triazole ligand. Since Zn(II) and Cd(II) ions as stable d^{10} electron configuration are highly resistant to redox process, the emission bands of both CPs are

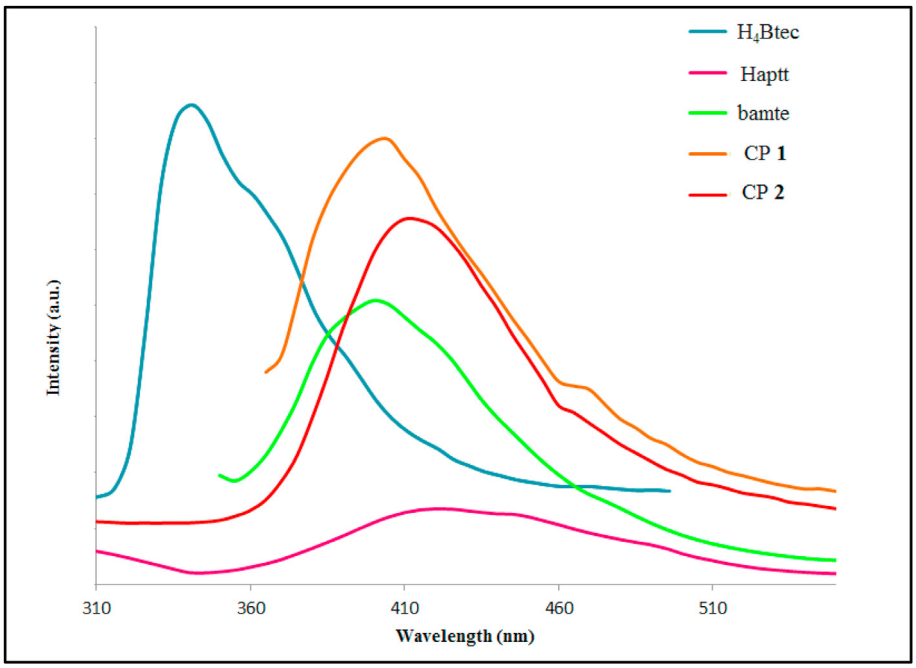

Fig. 9. The solid-state fluorescent emission spectra of H_4btec, Haptt, bamte, **CP1**, and at room temperature.

neither ligand to metal charge transfer (LMCT) nor metal to ligand charge transfer (MLCT) or metal to metal charge transfer (MMCT). Therefore, the observed shifts of the emission bands of both complexes should probably be assigned to the intra ligand fluorescent emission modified by metal coordination.

4. Conclusions

Two novel coordination polymers of d^{10} transition metals, namely $[Zn_2$ (bamte) (btec)$]_n$ (**CP1**) and $[Cd_3$ (aptt)$_2$ (btec)$]_n$ (**CP2**), utilizing flexible 1,2,4 triazole derivatives have been successfully synthesized under hydrothermal and solvothermal conditions, respectively. According to the determined molecular structures of **CP1** and **CP2**, both structures can be described as 3D pillar layered polymer networks. In both complexes, the corresponding, flexible 1,2,4 triazole moiety acts as a bridging agent (pillars) between the formed two dimensional M^{II} $btec^{4-}$ layers (M Zn and Cd), resulting in the formation of 3D coordination polymers having good thermal stability (up to *ca.* 250 °C). The stability of **CP1** may be due to the formed hydrogen bonds between the NH_2 groups of the 1,2,4 triazole moieties (pillars) and the oxygen atoms of the $btec^{4-}$ units (layers). The stability of **CP2** is not only due to the hydrogen bonds as observed in **CP1** but also to the strong π ··· π interactions between its five membered heterocycles and benzene rings.

Topologically, **CP1** can be classified as a binodal (4,6) connected 3D framework with $(4^4.6^{10}.8)$ $(4^4.6^2)$ Schlafli symbol possessing a rarely observed "*fsc*'' topology and **CP2** exhibits an unprecedented topology, namely a tetranodal (4,4,5,6) connected 3D framework with the point symbol of $\{(4^3.6^2.8)_2$ $(4^4.6^2)$ $(4^4.6^6)_2$ $(4^6.6^6.8^3)\}$. Solid state photoluminescence investigations on **CP1** reveals that the coordination polymer shows a slight red shift in its emission, whereas **CP2** exhibits a slight blue shift at room temperature compared with their corresponding 1,2,4 triazole ligands.

CRediT authorship contribution statement

Leila Heidari: preparation of the organic ligands and their corresponding metal complexes. **Mitra Ghassemzadeh:** Project administration, and funding, Conceptualization, writing, reviewing and editing of the final draft and revision of the manuscript. **Dieter Fenske:** crystallographic characterization and interpretation of the data, editing and reviewing of the manuscript. **Olaf Fuhr:** crystallographic characterization and interpretation of the data, editing and reviewing of the manuscript. **Farshid Mohsenzadeh:** writing, reviewing and editing of the final draft and revision of the manuscript. **Volodymyr Bon:** topological studies, editing and reviewing of the manuscript.

Declaration of competing interest

The authors declare that they have no known competing financial interests or personal relationships that could have appeared to influence the work reported in this paper.

Acknowledgements

This work was partly carried out with the support of the Karlsruhe Nano Micro Facility (KNMF), a Helmholtz Research Infrastructure at KIT. M. Ghassemzadeh and L. Heidari are grateful to thank Prof. Stefan Kaskel,[c] Dr. Irena Senkovska[c] and Bodo Felsner[c] for their helpful comments and suggestions that significantly improved this manuscript.

Appendix B. Supplementary data

Supplementary data to this article can be found online at https://doi.org/10.1016/j.jssc.2021.122011.

References

[1] J.H. Fu, H.J. Li, Y.J. Mu, H.W. Hou, Y.T. Fan, Chem. Commun. 47 (2011) 5271–5273.
[2] M.D. Allendorf, C.A. Bauer, R.K. Bhakta, R.J.T. Houk, Chem. Soc. Rev. 38 (2009) 1330–1352.
[3] Q.Y. Yang, P. Lama, S. Sen, M. Lusi, K.J. Chen, W.Y. Gao, M. Shivanna, T. Pham, N. Hosono, S. Kusaka, J.J. IV Perry, S. Ma, B. Space, L.J. Barbour, S. Kitagawa, M.J. Zaworotko, Angew. Chem. Int. 57 (2018) 5684–5689.
[4] Z. Chang, D.H. Yang, J. Xu, T.L. Hu, X.H. Bu, Adv. Mater 27 (2015) 5432–5441.
[5] Y.B. Zhang, W.X. Zhang, F.Y. Feng, J.P. Zhang, X.M. Chen, Angew Chem, Bar Int. 48 (2009) 5287–5290.
[6] J.H. Qin, Y.Y. Jia, H.J. Li, B. Zhao, D.Q. Wu, S.Q. Zang, H.W. Hou, Y.T. Fan, Inorg. Chem. 53 (2014) 685–687.
[7] J.P. Li, B.J. Li, M.T. Pan, B. Liu, J.J. Cheng, R.Y. Li, X.L. Gao, S.M. Wang, Cryst. Growth Des. 17 (2017) 2975–2986.

[8] Z.Q. Xu, Q. Wang, H.J. Li, W. Meng, Y. Han, H.W. Hou, Y.T. Fan, Chem. Commun. 48 (2012) 5736–5738.

[9] Z.Z. Xiao, L.J. Han, Z.J. Wang, H.G. Zheng, Dalton Trans. 47 (2018) 3298–3302.

[10] S.-Q. Wang, Q.Y. Yang, S. Mukherjee, D. O'Nolan, E. Patyk-Kazmierczak, K.-J. Chen, M. Shivanna, C. Murray, C.C. Tang, M.J. Zaworotko, Chem. Commun. 54 (2018) 7042–7045.

[11] Y.Q. Duan, J.H. Huang, S.C. Liu, T.T. Yu, J.P. Li, Y.P. Hao, Z.Y. Liu, B. Liu, Inorg. Chem. Commun. 81 (2017) 47–50.

[12] T.M. Smith, K. Perkins, D. Symester, S.R. Freund, J. Vargas, L. Spinu, CrystEngComm 16 (2014) 191–213.

[13] L.-J. Han, D. Zheng, S.-G. Chen, H.-G. Zheng, J. Ma, Small 14 (2018), 1703873.

[14] B.Y. Li, X.J. Zhou, Q. Zhou, G.H. Li, J. Hua, Y. Bi, Y.J. Li, Z. Shi, S.H. Feng, CrystEngComm 13 (2011) 4592–4598.

[15] Y. Yan, C. Li, Y. Wu, J. Gao, Q. Zhang, J. Mater. Chem. A 8 (2020) 15245–15270.

[16] L. Wang, H. Xu, J. Gao, J. Yao, Q. Zhang, Coord. Chem. Rev. 398 (2019), 213016.

[17] G. Férey, Dalton trans. (2009) 4400–4415.

[18] C.-K. Lin, D. Zhao, W.-Y. Gao, Z. Yang, J. Ye, T. Xu, Q. Ge, S. Ma, D.-J. Liu, Inorg. Chem. 51 (2012) 9039–9044.

[19] M.-L. Tong, X.-M. Chen, S.-R. Batten, J. Am, Chem. Soc. 125 (2003) 16170–16171.

[20] Y.-Q. Huang, Z.-L. Shen, T.-A. Okamura, Y. Wang, X.-F. Wang, W.-Y. Sun, J.-Q. Yu, N. Ueyama, Dalton trans. (2008) 204–213.

[21] G.-L. Li, G.-Z. Liu, L.-Y. Xin, X.-L. Li, L.-F. Ma, L.-Y. Wang, J. Inorg, Organomet. Polym 25 (2015) 694–701.

[22] L.-Y. Xin, G.-Z. Liu, L.-F. Ma, X. Zhang, L.-Y. Wang, Aust. J. Chem. 68 (2015) 758–765.

[23] G.-L. Li, W.-D. Yin, X.-L. Li, L.-Y. Xin, G.-Z. Liu, Synth. React. Inorg. Met. Org. Chem. 45 (2015) 869–874.

[24] L.-Y. Xin, G.Z. Liu, L.-F. Ma, L.-Y. Wang, J. Solid State Chem. 206 (2013) 233–241.

[25] R. Kitaura, K. Fujimoto, S. Noro, M. Kondo, S. Kitagawa, S. Angew Chem, Bar Int. 41 (2002) 133–135.

[26] G.-L. Li, G.-Z. Liu, L.-Y. Xin, L.-Y. Wang, CrystEngComm 14 (2012) 1729–1736.

[27] X. Zhang, L. Fan, W. Fan, B. Li, X. Zhao, CrystEngComm 17 (2015) 6681–6692.

[28] M. Arıcı, J. Solid State Chem. 262 (2018) 79–86.

[29] G.A. Senchyk, A.B. Lysenko, H. Krautscheid, E.B. Rusanov, A.N. Chernega, K.W. Kramer, S.-X. Liu, S. Decurtins, K.V. Domasevitch, Inorg. Chem. 52 (2013) 863–872.

[30] X.X. Wang, B.Y. Yu, K.V. Hecke, G.H. Cui, RSC Adv. 4 (2014) 61281–61289.

[31] D.-X. Hu, P.-K. Chen, F.L.L. Xue, Y.X. Che, J.-M. Zheng, Inorg. Chim. Acta. 360 (2007) 4077–4084.

[32] S. Sanda, S. Parshamoni, S. Konar, Inorg. Chem. 52 (2013) 12866–12868.

[33] J. Zhang, W. Jia, J. Wu, G. Tang, C. Zhang, New J. Chem. 43 (2019) 16078–16088.

[34] H. Furukawa, Y.B. Go, N. Ko, Y.K. Park, F.J. Uribe-Romo, J. Kim, M. O'Keeffe, O.M. Yaghi, Inorg. Chem. 50 (2011) 9147–9152.

[35] J.-P. Zhang, Y.-Y. Lin, X.-C. Huang, X.-M. Chen, J. Am, Chem. Soc. 127 (2005) 5495–5506.

[36] M. Du, Q. Wang, C.-P. Li, X.-J. Zhao, J. Ribas, Cryst. Growth Des. 10 (2010) 3285–3289.

[37] L.M. Fan, X.T. Zhang, Z. Sun, W. Zhang, Y.S. Ding, W.L. Fan, L.M. Sun, X. Zhao, H. Lei, Cryst. Growth Des. 13 (2013) 2462–2475.

[38] M. Ghassemzadeh, L. Fallahnedjad, M.M. Heravi, B. Neumüller, Polyhedron 27 (2008) 1655–1664.

[39] S. Bahemmat, M. Ghassemzadeh, B. Neumüller, Inorg. Chim. Acta. 435 (2015) 159–166.

[40] M. Ghassemzadeh, R. Firouzi, S. Shirkhani, S. Amiri, B. Neumüller, Polyhedron 69 (2014) 188–196.

[41] M. Ghassemzadeh, S. Bahemmat, M. Mahmoodabadi, B. Rezaii-Rad, H.H. Monfared, E. Mottefakeri, B. Neumüller, Polyhedron 29 (2010) 3036–3045.

[42] S. Bahemmat, M. Ghassemzadeh, M. Afsharpour, K. Harms, Polyhedron 89 (2015) 196–202.

[43] H.A. Habib, J. Sanchiz, C. Janiak, Inorg. Chim. Acta. 362 (2009) 2452–2460.

[44] W. Su, M. Hong, J. Weng, R. Cao, S.A. Lu, Angew Chem, Bar Int. 39 (2000) 2911–2914.

[45] T.S. Lobana, R. Sharma, R. Sharma, S. Mehra, A. Castineiras, P. Turner, Inorg. Chem. 44 (2005) 1914–1921.

[46] G. Aromí, L.A. Barrios, O. Roubeau, P. Gamez, Coord. Chem. Rev. 255 (2011) 485–546.

[47] Y. Yang, P. Du, Y. Liu, J.A. Ma, Cryst. Growth Des. 13 (2013) 4781–4795.

[48] O.V. Dolomanov, L.J. Bourhis, R.J. Gildea, J.A.K. Howard, H. Puschmann, J. Appl, Cryst 42 (2009) 339–341.

[49] G.M. Sheldrick, Acta Crystallogr. A71 (2015) 3–8.

[50] G.M. Sheldrick, Acta Crystallogr. C71 (2015) 3–8.

[51] V.A. Blatov, A.P. Shevchenko, D.M. Proserpio, Cryst. Growth Des. 14 (2014) 3576–3586.

[52] W.-H. Jiang, J.-L. Liu, L.-Z. Niu, B. Liu, Y.-H. Yu, G.-F. Hou, D.-S. Ma, Polyhedron 124 (2017) 191–199.

[53] Y.-Q. Zhang, V.A. Blatov, X.-X. Lv, C.-H. Yang, L.-L. Qian, K. Li, B.-L. Li, B. Wu, Polyhedron 155 (2018) 223–231.

[54] P. Ju, E.-S. Zhang, X. Liu, L. Jiang, Inorg. Chem. Commun. 111 (2020), 107641.

[55] J.Y. Gao, N. Wang, X.H. Xiong, C. Chen, W. Xie, CrystEngComm 15 (2013) 3261–3270.

[56] L. Ma, Y. Liu, F. Su, J. Solid state chem. 269 (2019) 65–71.

[57] J.-X. Yang, X. Zhang, Y.-Y. Qin, Y.-G. Yao, Cryst. Growth Des. 20 (2020) 6366–6381.

[58] F. Zou, W.-M. Xuan, X.-M. Fang, H. Zhang, o213, Acta Crystallogr. E64 (2008).

[59] L. Li, W. Li, S. Yang, L. Wei, Ch. Wang, H. Hou, J. Coord. Chem. 66 (2013) 2948–2956.

[60] G. Liu, Y. Li, J. Chi, N. Xu, X. Wang, H. Lin, B. Chen, J. Li, Dalton Trans. 49 (2020) 737–749.

[61] L. Lu, J. Wanga, S. Zhou, Y. Zhong, Y. Sun, X. Wub, A. Singh, A. Kumar, Inorg. Chim. Acta. 508 (2020), 119647.

[62] H.-T. Wu, H.-P. Li, S.-N. Li, Y.-C. Jiang, M.-C. Hu, Q.-G. Zhai, J. Solid State Chem. 283 (2020), 121166.

[63] G. Yuan, C. Zhang, D.-J. Xu, K.-Z. Shao, X.-M. Li, X.-R. Hao, Z.-M. Su, Polyhedron 180 (2020), 114430.

[64] Q. Huang, J.-H. Huang, L. Gu, J.-X. Ruan, Y.-H. Yu, J.-S. Gao, RSC Adv. 8 (2018) 557–566.

[65] S. Zhao, X.-X. Lv, L.-L. Shi, B.-L. Li, B. Wu, RSC Adv. 6 (2016) 56035–56041.

[66] Y.F. Wang, Zh. Li, Y.C. Sun, J.S. Zhao, L.Y. Wang, CrystEngComm 15 (2013) 9980–9987.

[67] Q. Ye, X.B. Chen, Y.M. Song, X.S. Wang, Inorg. Chim. Acta. 358 (2005) 1258–1262.

[68] C. Janiak, J. Chem. Soc., dalton trans. (2000) 3885–3896.

[69] W.Q. Kan, J. Yang, Y.-Y. Liu, J.F. Ma, Inorg. Chem. 51 (2012) 11266–11278.

[70] B. Xu, J. Lv, R. Cao, Cryst. Growth Des. 9 (2009) 3003–3005.

[71] X. Shi, G. Zhu, Q. Fang, G. Wu, G. Tian, R. Wang, D. Zhang, Eur. J. Inorg. Chem (2004) 185–191.